

# 1 Magnetic Anisotropy of Single Mn Acceptors in GaAs in an External Magnetic Field

2 M. Bozkurt,<sup>1,\*</sup> M.R. Mahani,<sup>2</sup> P. Studer,<sup>3,4</sup> J.-M. Tang,<sup>5</sup> S.R. Schofield,<sup>3,6</sup> N.J. Curson,<sup>3,4</sup>  
 3 M.E Flatté,<sup>7</sup> A. Yu. Silov,<sup>1</sup> C.F. Hirjibehedin,<sup>3,6,8</sup> C.M. Canali,<sup>2</sup> and P.M. Koenraad<sup>1</sup>

4 <sup>1</sup>*Photonics and Semiconductor Nanophysics, Department of Applied Physics, Eindhoven University  
 5 of Technology, P. O. Box 513, NL-5600 MB Eindhoven, The Netherlands*

6 <sup>2</sup>*School of Computer Science, Physics and Mathematics, Linnaeus University, 391 82 Kalmar, Sweden*

7 <sup>3</sup>*London Centre for Nanotechnology, University College London (UCL), London, WC1H 0AH, U.K.*

8 <sup>4</sup>*Department of Electronic and Electrical Engineering, UCL, London, WC1E 7JE, UK*

9 <sup>5</sup>*Department of Physics, University of New Hampshire, Durham, New Hampshire 03824-3520, U.S.A.*

10 <sup>6</sup>*Department of Physics and Astronomy, UCL, London, WC1E 6BT, UK*

11 <sup>7</sup>*Department of Physics and Astronomy, University of Iowa, Iowa City, Iowa 52242-1479, U.S.A.*

12 <sup>8</sup>*Department of Chemistry, UCL, London, WC1H 0AJ, UK*

13 (Dated: September 20, 2018)

We investigate the effect of an external magnetic field on the physical properties of the acceptor hole states associated with single Mn acceptors placed near the (110) surface of GaAs. Cross-sectional scanning tunneling microscopy images of the acceptor local density of states (LDOS) show that the strongly anisotropic hole wavefunction is not significantly affected by a magnetic field up to 6 T. These experimental results are supported by theoretical calculations based on a tight-binding model of Mn acceptors in GaAs. For Mn acceptors on the (110) surface and the subsurfaces immediately underneath, we find that an applied magnetic field modifies significantly the magnetic anisotropy landscape. However the acceptor hole wavefunction is strongly localized around the Mn and the LDOS is quite independent of the direction of the Mn magnetic moment. On the other hand, for Mn acceptors placed on deeper layers below the surface, the acceptor hole wavefunction is more delocalized and the corresponding LDOS is much more sensitive on the direction of the Mn magnetic moment. However the magnetic anisotropy energy for these magnetic impurities is large (up to 15 meV), and a magnetic field of 10 T can hardly change the landscape and rotate the direction of the Mn magnetic moment away from its easy axis. We predict that substantially larger magnetic fields are required to observe a significant field-dependence of the tunneling current for impurities located several layers below the GaAs surface.

**PACS numbers:** 75.50.Pp

## 14 I. INTRODUCTION

15 Magnetic semiconductors have attracted strong atten-  
 16 tion in the last decade because of their potential to  
 17 combine opto-electronic and magnetic properties in spin-  
 18 tronic devices. The most commonly investigated material  
 19 as a magnetic semiconductor is GaAs doped with tran-  
 20 sition metal Mn-impurities. Mn acts as an acceptor in  
 21 GaAs and its magnetic properties are mainly determined  
 22 by the magnetic moment of the half filled d-shell [1]. In  
 23 highly Mn doped GaAs, the observed ferromagnetism in  
 24 GaMnAs has been shown to be hole mediated [2, 3], as a  
 25 result of exchange coupling between the p-like acceptor  
 26 holes residing in the valence band and the electrons in the  
 27 d-shell which we will refer to as the Mn core from now on.  
 28 On the other hand, for applications in spintronic devices,  
 29 it is important to investigate methods to read, set and  
 30 manipulate the magnetic orientation of the Mn core, es-  
 31 pecially at the level of a single Mn impurity. Spectacular  
 32 results have been achieved with optical polarization and  
 33 manipulation of low Mn doped GaAs/AlGaAs quantum  
 34 wells [4] and single Mn doped quantum dots [5, 6]. Other  
 35 important work in the field of single spin reading and

36 manipulation has been done for single nitrogen-vacancy  
 37 centers in diamond [7].

38 In this paper, we investigate low-concentration Mn-  
 39 doped GaAs. Because Mn has strongly coupled mag-  
 40 netic and electric properties, spin manipulation by elec-  
 41 tric fields has been suggested as a possibility in addition  
 42 to manipulation by magnetic and optical fields. Cross-  
 43 sectional scanning tunneling microscopy (X-STM) has  
 44 been used in the past to study the Mn acceptor wave  
 45 function at the atomic scale and to manipulate its charge  
 46 state. The experimental study of the Mn acceptor wave-  
 47 function by X-STM showed a strongly anisotropic shape  
 48 of the acceptor wavefunction [8] as was predicted by tight  
 49 binding calculations [9]. These experimental and theo-  
 50 retical results proved that the observed anisotropy of the  
 51 acceptor wavefunction is due to the cubic symmetry of the  
 52 GaAs crystal. Additional studies showed that the  
 53 anisotropy of the Mn acceptor wavefunction is also in-  
 54 fluenced by (local) strain due to a nearby InAs quantum  
 55 dot [10] or the relaxation of the surface [11].

56 These results indicate that STM can also be an excel-  
 57 lent tool to investigate the effects of the orientation of the  
 58 magnetic moment of the Mn core on the acceptor wave-  
 59 function. In fact, theoretical work [12],[13] has predicted  
 60 that the local density of states (LDOS) of the acceptor-  
 61 hole wavefunction can depend strongly on the direction

---

\* E-mail:Bozkurt.Murat.2010@gmail.com

of the Mn moment. Since the LDOS is directly related to the tunneling current, these predictions suggest that it might be possible to control the STM electric current by manipulating the individual Mn core spin, for example with an external magnetic field. An X-STM and X-STs study of the energetic level of Mn close to the GaAs [110] cleavage surface has already shown that the 3-fold degeneracy of the  $J=1$  ground level is split because of the reduced symmetry [14]. Magnetic-field manipulation and control of atomic spins is presently undergoing fast progress, showing great promise to selectively address individual atoms [15]. Control of atomic spin, combined with the aforementioned sensitivity of the STM current on the dopant magnetic moment direction, could be a crucial step in realizing multifunctional spin-electronic devices based on individual atoms. Apart from addressing electrical properties of single magnetic dopants, STM has been shown to be also well capable of positioning individual dopants within a semiconductor surface [16, 17].

In this paper we will use STM to explore the effect of an external magnetic field on the magnetic orientation of the magnetic moment of a single Mn impurity in dilute Mn doped GaAs and compare the results with tight-binding model calculations. In Section II we present a review of the theoretical work that has been published in 2 papers [12],[13]. These calculations are based on a tight binding model and show that a change in the spin orientation of the Mn core can sometimes give rise to a detectable change in LDOS of the Mn acceptor wavefunction. In Section III we present experimental results of STM measurements on single Mn impurities in GaAs in a magnetic field. We will show that the LDOS of the Mn acceptor wavefunction is not significantly modified by magnetic fields up to 6 Tesla. In Sections IV and V we present theoretical results of tight binding modelling of Mn in GaAs where a magnetic field has been explicitly included in the Hamiltonian. These calculations support our experimental observations and show that a dependence of LDOS on external magnetic is in fact expected only for Mn acceptors placed several layers below the GaAs (110) and can be detected only with stronger magnetic fields than the ones presently available.

## II. REVIEW

Tang et al. [12] and Strandberg et al. [13] have reported results of calculations of the dependence the Mn acceptor hole wavefunction on the orientations of the Mn magnetic moment. The paper by Tang et al. [12] describes the Mn LDOS in bulk GaAs with an  $sp^3$  tight binding model in which the Mn core spin is taken in calculation by a spin dependent term in the potential at the four nearest neighbor sites in a zinc-blende crystal. It is found that the energy spectrum of the Mn is independent of the Mn core spin orientation. However, the LDOS of the Mn is found to be depending on the Mn spin orientation. A qualitative description of this depen-

dence is given in terms of spin-orbit coupling between the spin of the Mn core and the orbital character of the Mn acceptor hole. In absence of spin-orbit interaction, the LDOS of the Mn acceptor state would have the same  $T_d$  symmetry as the surrounding zinc-blende crystal. However, the spin-orbit coupling is taken into account and the symmetry of the Mn acceptor wavefunction is reduced. The contour surface of the acceptor LDOS for various Mn core spin directions show that in general, the LDOS has an oblate shape with the short axis aligned with the Mn core spin axis. For a quantitative comparison with X-STM experiments, cross sectional views of the LDOS are calculated in the (110) plane. The largest variation in the cross sectional images of the LDOS is seen when the Mn core spin direction changes from [001] or  $[1\bar{1}0]$  to [110]. A variation in LDOS of up to 90% is predicted by these tight binding calculations when the Mn core spin switches from parallel to perpendicular to the (110) surface. There is also a small difference of 15% in the LDOS when the Mn core spin is aligned in the two directions parallel to the (110) plane. When the spin of Mn core can be changed with an external magnetic field and possibly with ESR techniques [15, 18], the differences in the LDOS are expected to be visible in an X-STM experiment.

This model gives a good description of Mn in bulk GaAs but the effect of the cleavage surface is completely neglected. In fact it has been shown experimentally[11] that the wavefunction of a Mn near the (110) cleavage surface can be strongly affected by the strain from the surface relaxation. In the same paper, bulk tight binding calculations support the observation of a broken symmetry near the surface. The surface is taken into account by applying a uniform strain to the bulk model by shifting the Ga lattice with respect to the As lattice. The calculation results presented in that paper are the average of different Mn core spin orientations. In Fig. 1, the same results are presented but for individual Mn core spin orientations. Fig. 1 was unpublished in this form. A clear difference in LDOS can be observed when the Mn core spin changes its orientation from the hard axis to the easy axis.

In the paper by Strandberg et al. [13] the reconstructed surface is taken into account for the calculation of the LDOS dependence of the Mn acceptor state on the Mn core spin orientation using a tight binding model which includes the exchange interaction, spin-orbit coupling and Coulomb interaction. This makes a direct comparison with X-STM experiments more justified and the results indeed show the same experimentally observed breaking of the symmetry of the wavefunction due to the near presence of the surface. In Ref. 13 Mn acceptors in bulk GaAs (neglecting the surface) have also been considered. For Mn in bulk GaAs, the energy level of the Mn state calculated for different orientations of the Mn core spin shows a small magnetic anisotropy, in contrast to the results of Ref. 12, where no magnetic anisotropy was found for Mn in bulk. The easy axis in Ref. 13 for the Mn core spin is oriented along the [001] direction

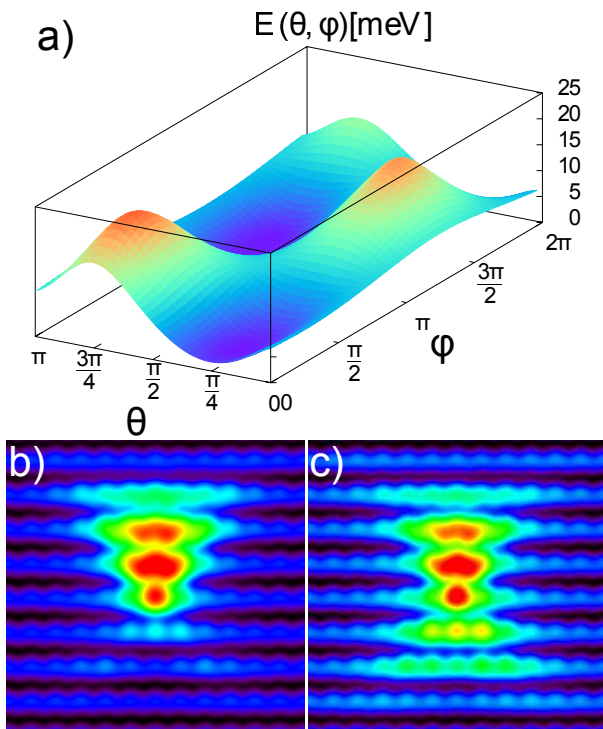


FIG. 1. (a) Magnetic Anisotropy Energy (MAE) of a Mn acceptor according to a tight binding calculation for strained bulk material. The energy level difference between the easy and the hard axis is about 23 meV, based on a uniform strain estimated in Ref. [11]. The angles  $\theta$  and  $\phi$  have the same definition as in Fig. 4. (b) Mn LDOS at five atomic layers from the Mn position when the core spin is oriented along the (b) easy axis or (c) hard axis.

176 whereas the hard axis is found to be lying in the (001)  
 177 plane. The energy barrier between the hard axis and the  
 178 easy axis is found to be 4.35 meV which is very small  
 179 in comparison with the Mn binding energy in GaAs (113  
 180 meV). At first, the presence of a magnetic anisotropy is  
 181 surprising since there is no difference between the [001]  
 182 and [010] or [100] directions in a Zinc-Blende crystal.  
 183 The observed anisotropy can be explained by the use of  
 184 periodic boundary conditions on finite clusters used in  
 185 this paper [13]. The influence of other Mn atoms in the  
 186 area may indeed introduce a small magnetic anisotropy  
 187 and thus the observed magnetic anisotropy of Mn in bulk  
 188 GaAs is artificial. Indeed, more recent calculations carried  
 189 out on much larger clusters show that the bulk  
 190 magnetic anisotropy decreases monotonically with cluster  
 191 size, down to a fraction of a meV for the largest clusters  
 192 of 40,000 atoms [19].

193 On the other hand, the calculation of the LDOS for  
 194 Mn in bulk GaAs in Ref. [13] shows good similarity with  
 195 the calculations in Ref. [12]. The LDOS is found to be  
 196 spreading in the direction perpendicular to the Mn core  
 197 spin axis. The change in the shape of the LDOS is explained  
 198 in terms of the  $p_x$ ,  $p_y$  and  $p_z$  character of the  
 199 Mn acceptor hole. For different orientations of the Mn

200 core spin, different components in the character domi-  
 201 nate. When the Mn core spin direction is changed from  
 202  $[1\bar{1}0]$  to  $[110]$  a drop in LDOS of 74% is observed at 4  
 203 atomic layers from the Mn position. This drop in LDOS  
 204 is 25% when the core spin direction changes from  $[1\bar{1}0]$   
 205 to  $[001]$ , which is again in good agreement with the other  
 206 calculations in [12].

207 In Ref. 13 similar calculations have been done for Mn  
 208 in or below the GaAs (110) surface layer. For Mn at the  
 209 surface and the first subsurface layer, a strong localiza-  
 210 tion of the LDOS is observed and a magnetic easy axis in  
 211 the  $[111]$  direction is found. The difference in LDOS for  
 212 different Mn core spin orientations is negligible. Thus in  
 213 an X-STM experiment, we expect to see no effect of the  
 214 magnetic field on the Mn atoms very close to the surface.

215 For Mn atoms deeper below the (110) surface,  
 216 the LDOS becomes more extended and the magnetic  
 217 anisotropy shows a complex behavior for subsequent  
 218 depths. However, from the fourth layer beneath the (110)  
 219 surface and deeper, one can recognize the emergence of  
 220 an easy plane with its normal in the  $[1\bar{1}0]$  direction. The  
 221 anisotropy energy is found to be at least 15 meV. Images  
 222 of the (110) surface LDOS show that there is an increas-  
 223 ing difference in LDOS for an increasing depth when the  
 224 Mn core spin changes from the easy axis to the hard  
 225 axis. For Mn atoms placed on fourth subsurface layers  
 226 and deeper, the difference in LDOS varies between 40%  
 227 and 82%.

228 In summary, both Refs. 12 and 13 have treated the  
 229 behavior of the Mn acceptor hole LDOS in the (110)  
 230 plane for different Mn core spin orientations. In both  
 231 papers it is found that when the Mn core spin direction  
 232 is changed from  $[1\bar{1}0]$  to  $[110]$ , a drastic change in the  
 233 LDOS is taking place. The inclusion of the cleavage sur-  
 234 face relaxation has resulted in similar observations.

235 The mechanism for the magnetic anisotropy in Refs. 12  
 236 and 13 is the same — the presence of the surface, or  
 237 strain, lowers the energy of an orbital wave function with  
 238 quantization axis along a specific direction, and the spin-  
 239 orbit interaction (which correlates the spin axis with the  
 240 orbital axis) causes that preferred orbital direction to  
 241 select a preferred spin axis. The effective energy asso-  
 242 ciated with the correlation between spin axis and orbi-  
 243 tal axis is of the same order as the binding energy  
 244 (Refs. 9, 12, and 13 found it to be  $\sim 40$  meV). At mag-  
 245 netic fields required to overcome the magnetic anisotropy  
 246 energy the magnetic length is of order 3 nm, which is  
 247 three times larger than the effective Bohr radius of the  
 248 acceptor ( $\sim 1$  nm). Therefore the overall distortion of  
 249 the acceptor state wave function due to the direct effect  
 250 of the magnetic field on the orbital wave function is small  
 251 compared with the spin-orbit term. What is not certain,  
 252 however, is whether the effect of the magnetic field on the  
 253 acceptor state wave function can substantially change the  
 254 magnetic anisotropy; this will be examined in Section V.

255 In an X-STM experiment, one can also check the re-  
 256 sults of these calculations by applying a magnetic field  
 257 perpendicular and parallel to the (110) cleavage plane

258 and by measuring the Mn contrast, which can change  
 259 with a factor as high as 90%. In the next section, we dis-  
 260 cuss the X-STM experiments that have been performed  
 261 to observe the predicted effects.

### 262 III. EXPERIMENTS

263 A Mn doped layer of 500 nm thick was grown on a  
 264 p-type GaAs substrate at high temperature with Mn  
 265 concentrations of about  $3 \times 10^{19} \text{ cm}^{-3}$ . The experiments  
 266 are performed with an Omicron Cryogenic STM operat-  
 267 ing at a base temperature of 2.5 K. A magnetic field  
 268 vector can be applied with fields of up to 6 T in the  
 269 z-direction only or max. 2 T in the z-direction together  
 270 with max. 1 T in the x- and y-directions. The x-, y- and  
 271 z-direction are indicated in figure 2a where 2 Mn atoms  
 272 at different depths below the cleaved surface are visible.  
 273 The magnetic field is indicated in the vector notation in  
 274 units of T:  $\vec{B} = (B_x, B_y, B_z)$ .

275 From Ref. [11], we estimate that Mn A is approximately  
 276 8 atomic layers below the cleavage surface and that Mn  
 277 B is at about 5 atomic layers below the cleavage surface.  
 278 In [13], a change in contrast of 40% is predicted for a  
 279 Mn A at 8 layers below the cleavage surface when the  
 280 Mn core spin changes from the [110] direction to the  
 281  $[1\bar{1}0]$  direction. For Mn B at 5 atomic layers beneath  
 282 the cleavage surface, a change of 60% is predicted  
 283 when the Mn core spin direction changes from the [110]  
 284 direction to the  $[1\bar{1}0]$  direction. As can be seen from  
 285 the comparison of figures 2a and 2b, there is no change  
 286 at all in the Mn contrast for both Mn atoms when the  
 287 magnetic field is changed from 1 T in the y direction to  
 288 -6 T in the z-direction. In figure 3, a more quantitative  
 289 comparison is made by looking at the contrast of the Mn  
 290 atoms in different magnetic fields through the dashed  
 291 lines in figure 2b. Also in these plots, it can be seen that  
 292 for both Mn atoms, there is no difference at all in the  
 293 contrast for different orientations of the magnetic field.

294 For Mn B, the plots for  $B=(0,1,0)$  and  $B=(0,0,-6)$  are  
 295 slightly different from the rest because of a small tip  
 296 modification that has taken place. The tip has become  
 297 slightly less sharp in the scan direction (the [001]  
 298 x-direction) and this difference is noticed when sharper  
 299 objects like Mn B are imaged. Mn A has FWHM of  
 300 about 4.5 nm in the scan direction, while Mn B has a  
 301 sharper feature with a FWHM of about 2.0 nm. The  
 302 different FWHM of the Mn features has been related to  
 303 the depth below the GaAs surface [11]

### 304 IV. THEORETICAL MODEL

305 We model theoretically substitutional Mn impuri-  
 306 ties in GaAs following the procedure put forward in  
 307 Ref. 13. Our second-quantized tight-binding Hamilto-

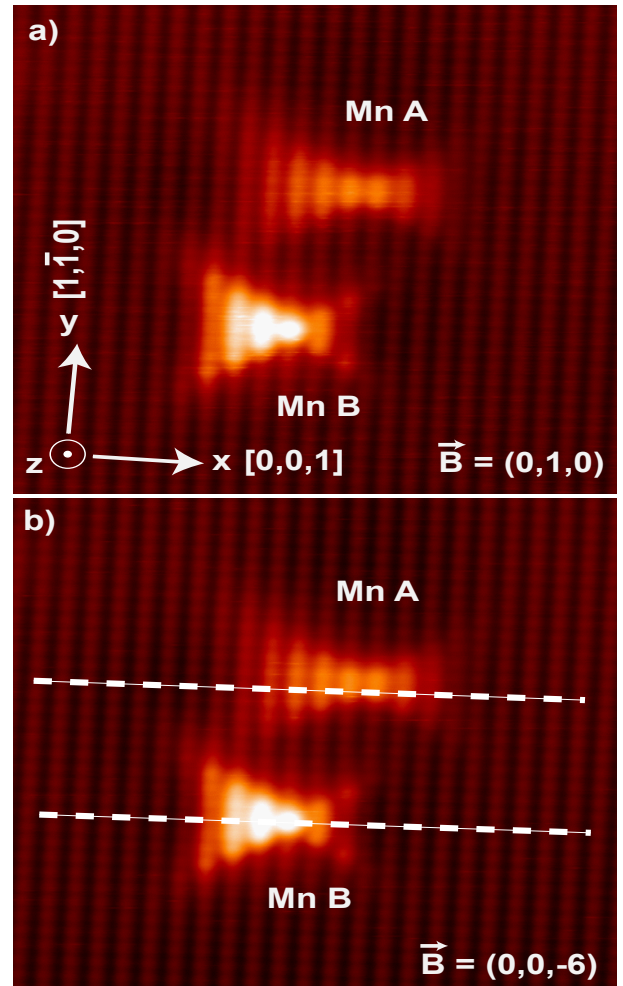


FIG. 2. 13x13 nm X-STM images of two Mn atoms at differ-  
 ent depths below the (110) cleavage plane. The x direction  
 corresponds with the crystallographic [001] direction and the  
 y-direction corresponds with the  $[1\bar{1}0]$  direction. The images  
 are taken at +1.4 V and 50 pA at a temperature of about  
 2.5 K. In a) a magnetic field of 1 T is oriented in the  $[1\bar{1}0]$   
 y-direction and in b) a magnetic field of -6 T is oriented in  
 the  $[110]$  z-direction.

nian for (Ga,Mn)As takes the following form:

$$\begin{aligned}
 H = & \sum_{ij, \mu\mu', \sigma} t_{\mu\mu'}^{ij} a_{i\mu\sigma}^\dagger a_{j\mu'\sigma} + J_{pd} \sum_m \sum_{n[m]} \vec{S}_n \cdot \hat{\Omega}_m \\
 & + \sum_{i, \mu\mu', \sigma\sigma'} \lambda_i \langle \mu, \sigma | \vec{L} \cdot \vec{S} | \mu', \sigma' \rangle a_{i\mu\sigma}^\dagger a_{i\mu'\sigma'} \\
 & + \frac{e^2}{4\pi\epsilon_0\epsilon_r} \sum_m \sum_{i\mu\sigma} \frac{a_{i\mu\sigma}^\dagger a_{i\mu\sigma}}{|\vec{r}_i - \vec{R}_m|} + V_{\text{Corr}}, \quad (1)
 \end{aligned}$$

308 where  $i$  and  $j$  are atomic indices that run over all atoms,  
 309  $m$  runs over the Mn, and  $n[m]$  over the nearest neighbors  
 310 of Mn atom  $m$ .  $\mu$  and  $\nu$  are orbital indices and  $\sigma$  is a  
 311 spin index. The first term in Eq. (1) contains the near-  
 312 neighbor Slater-Koster tight-binding parameters[20, 21]  
 313 that reproduce the band structure of bulk GaAs[22] and

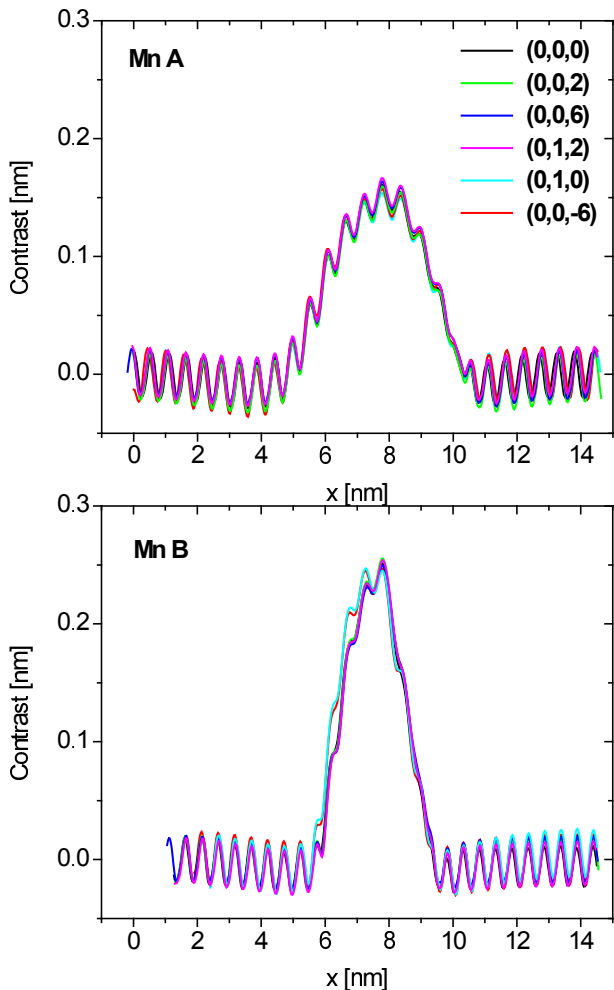


FIG. 3. a) Contrast of Mn A along the [001] direction indicated with a dashed line in figure 2b. b) same plot for Mn B. Mn A has FWHM of about 4.5 nm and Mn B has a FWHM of about 2.0 nm

that are rescaled[13, 23, 24] when needed to account for the buckling of the (110) surface.

The second term implements the antiferromagnetic exchange coupling between the Mn spin  $\hat{\Omega}_m$  (treated as a classical vector) and the nearest neighbor As  $p$ -spins  $\vec{S}_n = 1/2 \sum_{\pi\sigma\sigma'} a_{n\pi\sigma}^\dagger \vec{\tau}_{\sigma\sigma'} a_{n\pi\sigma'}$ . The exchange coupling  $J_{pd} = 1.5$  eV has been inferred from theory [25] and experiment [26]. As a result of this term the acceptor hole that is weakly bound to the Mn will become spin polarized. This model contains only  $s$  and  $p$  orbitals, and the effect of the Mn  $3d^5$  electrons is encoded in the exchange term.

Next, we include an on-site spin-orbit one-body term, where the renormalized spin-orbit splittings are taken from Ref. 22. Spin-orbit coupling will cause the total energy to depend on the Mn spin direction, defined by a collinear variation of  $\hat{\Omega}_m$ .

The fourth term is a long-range repulsive Coulomb part

that is dielectrically screened by the host material. To account in a simple way for weaker dielectric screening at the surface, the dielectric constant  $\epsilon_r$  for a Mn on the surface is reduced from the bulk GaAs value 12 to 6 for the affected surface atoms. This crude choice is qualitatively supported by experimental results [17, 27].

The last term  $V_{\text{CORR}}$  is a one-particle correction potential for the Mn central cell. This term is the least known and understood theoretically. It consists of on- and off-site parts,  $V_{\text{CORR}} = V_{\text{on}} + V_{\text{off}}$  which influence the Mn ion and its As nearest neighbors respectively. The on-site Coulomb correction is estimated to be 1.0 eV from the ionization energy of Mn. The off-site Coulomb correction affects all the nearest-neighbor As atoms surrounding the Mn ion and together with the exchange interaction, it reflects primarily the  $p$ - $d$  hybridization physics and is the parameter that in the model primarily controls the binding energy of the hole acceptor state. The off-site Coulomb correction value is set by tuning the position of the Mn-induced acceptor level in the bulk to the experimentally observed position [28–31] at 113 meV above the first valence band level. The value thus obtained is  $V_{\text{off}} = 2.4$  eV. When the Mn impurity is on the GaAs surface, the value of  $V_{\text{off}}$  is reduced to ensure that the position of the acceptor level is consistent with the value attained via STM spectroscopy.

The off-site Coulomb correction is in fact a repulsive potential for the electrons. If we use the bulk value (2.4 eV) for the surface, the acceptor level lies deep in the gap at 1.3 eV above the valence band, which means the acceptor wave function is now much more localized around the Mn than its bulk counterpart. In order to guarantee the experimentally observed position for the acceptor level, 0.85 eV [16], we have to decrease this repulsive potential for the electrons, which causes the hole wave function to be less localized with a corresponding smaller binding energy.

The electronic structure of GaAs with a single substitutional Mn atom is obtained by performing a super-cell type calculation with a cubic cluster of a few thousands atoms and periodic boundary conditions in either 2 or 3 dimensions, depending on whether we are studying the (110) surface or a bulk-like system. The (110) surface of GaAs is simplified from both theoretical and experimental points of view, by the absence of large surface reconstruction. In order to remove artificial dangling-bond states that would otherwise appear in the band gap, we include relaxation of surface layer positions following a procedure introduced in Refs. [23 and 24]. For more details the reader is referred to Ref. [13].

We would like to emphasize that the strength of the off-site Coulomb correction is the only important fitting parameter of the model, and its value is fixed once for all by the procedure described above. All the other parameters in Eq. 1 are either determined by theoretical considerations, or for the cases when this is not possible (e.g. short-range onsite potential) their values are extracted from experiment. In any case, they affect weakly

390 the properties of the acceptor level. Once the parameters of the Hamiltonian of Eq. 1 are chosen in the way  
 391 indicated above, the model has to be viewed as a microscopic description, with predictive power, of the properties  
 392 of Mn impurities in GaAs surfaces and subsurfaces. In this sense the model of Ref. 13 has been quite successful  
 393 in capturing some of the salient features of the STM experiments [14, 32], probing the Mn-dopant acceptor hole near the GaAs (110) surface. For example, it  
 394 correctly describes the dependence of the acceptor binding energy [14] and the shape of the hole wave function [32] on the layer depth below the surface on which the magnetic dopant is positioned. The model also makes a  
 395 prediction on how the magnetic anisotropy barrier for the Mn-impurity-hole magnetic complex changes as a function of the layer depth. These predictions can be indirectly checked by the magnetic-field studies that are the  
 396 main scope of the present paper.

397 In order to study the response of the system to an external magnetic field, we introduce the Zeeman term  
 398

$$H_z = -\frac{\mu_B}{\hbar} \sum_i \sum_{\mu\mu'\sigma\sigma'} \left\langle \mu\sigma \left| (\vec{L} + g_s \vec{S}) \cdot \vec{B} \right| \mu'\sigma' \right\rangle a_{i\mu\sigma}^\dagger a_{i\mu'\sigma'} - g_s \frac{\mu_B}{\hbar} \sum_m \hat{\Omega}_m \cdot \vec{B}, \quad (2)$$

399 where the first term runs over all  $s$  and  $p$  orbitals of all atoms, and the second term represents the coupling of the magnetic field with the magnetic moment of the Mn impurities, treated as a classical vector. Here  $\mu_B = \frac{\hbar e}{2m} = 5.788 \times 10^{-2} \text{ meV T}^{-1}$  is the Bohr magneton,  $g_s = 2$ , and we follow the incorrect but common convention that spins and magnetic moments are parallel to each other [33]. Therefore in the paper we will loosely refer to the direction of  $\hat{\Omega}$  as the direction of the Mn magnetic moment.

## 400 V. THEORETICAL RESULTS AND DISCUSSION

401 We start by analyzing the magnetic anisotropy properties for one Mn at the (110) GaAs surface layer and the immediate subsurface layers, and see how these are modified by the presence of an external magnetic field of a few Tesla. The magnetic anisotropy landscape as a function of  $\hat{\Omega}$  for one Mn at the surface and the first 9 subsurfaces has been studied in detail in Ref. 13. Typically the system has an uniaxial anisotropy with two minima separated by an energy barrier. We will refer to the  $\hat{\Omega}$  direction of minimum energy as the *easy* direction and the one of maximum energy as the *hard* direction.

402 We first consider the case of one Mn impurity at the (110) surface. To facilitate the comparison with the case in which a magnetic field is present, we recalculated and plotted here anisotropy landscapes and LDOS in the absence of the magnetic field, originally published in Ref. 13, using an improved code.

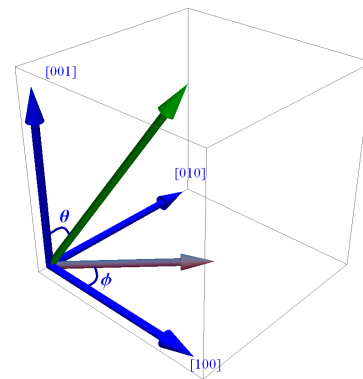


FIG. 4. Color online – The direction of  $\theta$  and  $\phi$  with respect to the crystal axis.

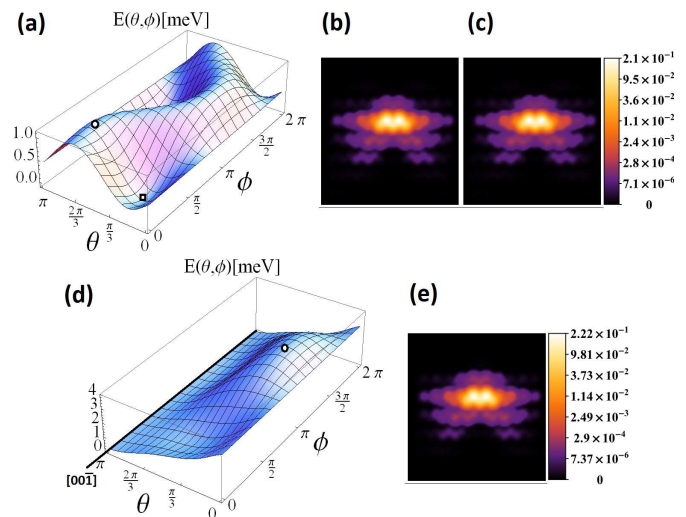


FIG. 5. Color online – The magnetic anisotropy energy (MAE) landscape and the Mn-acceptor-level local density of states (LDOS) for one Mn at the [110] surface. (a) The MAE in the absence of an external magnetic field, as a function of the angles  $\theta$  and  $\phi$  defining the direction of the Mn spin  $\hat{\Omega}$ . The barrier (hard) direction is marked with a circle and the minimum energy (easy direction) with a square. (b) and (c) LDOS of the Mn acceptor level when the Mn magnetic moment points in the easy and hard direction respectively, as defined in panel (a). (d) The MAE in the presence of a 6 T external magnetic field applied along the hard direction ( $\theta = 3\pi/4, \phi = \pi/4$ ). (e) The LDOS in the presence of a 6 T magnetic field. Here the Mn magnetic moment is along the easy direction determined by the landscape (d) modified by the presence of the external field. The barrier (hard) direction is marked with a circle and the minimum energy (easy direction) with a solid line.

439 In Fig. 5(a) we plot the anisotropy energy landscape in the absence of the magnetic field, as a function of the angles  $\theta$  and  $\phi$  defining the direction of  $\hat{\Omega}$ . The coordinate system used for this and the other plots in the paper has  
 440  $\theta = 0$  parallel to the [001] axis, ( $\theta = \pi/2, \phi = 0$ ) parallel  
 441 to [100], and ( $\theta = \pi/2, \phi = \pi/2$ ) parallel to [010]. See

445 Fig. 4.

446 The anisotropy landscape displays two minima, identi-  
 447 fying the easy direction [111], separated by an energy bar-  
 448 rier of the order of 1 meV. Note that these tight-binding  
 449 results of the magnetic anisotropy of a Mn at the (110)  
 450 GaAs surface are consistent with recent first-principles  
 451 estimates[34]. Panels (b) and (c) of Fig. 5 show the LDOS  
 452 for the Mn acceptor state when the Mn spins point along  
 453 the easy and hard direction respectively, determined from  
 454 the landscape in (a). As discussed in Sec. II and shown  
 455 clearly in the figures, the acceptor state wavefunction for  
 456 a Mn on the surface is very localized around the impurity,  
 457 and the dependence of the LDOS on the Mn spin orienta-  
 458 tion is negligible. The acceptor wavefunction, itself  
 459 strongly anisotropic, seems to be completely decoupled  
 460 from the orientation of the Mn magnetic moment.

461 Fig. 5(d) and (e) show the effect of a 6 T magnetic  
 462 field on the anisotropy and LDOS respectively, when the  
 463 field is applied in the hard direction of the anisotropy  
 464 landscape in (a).

465 We can see that the magnetic field changes consider-  
 466 ably the anisotropy landscape, which has now an easy  
 467 axis at  $\theta = \pi$  (the direction of the field). Note that in  
 468 the presence of the field the anisotropy barrier has in-  
 469 creased up to 4 meV. The LDOS in Fig. 5(e) is now  
 470 calculated for  $\hat{\Omega}$  pointing along the new easy axis, deter-  
 471 mined by the magnetic field. Despite the strong change  
 472 in the anisotropy landscape brought about by the mag-  
 473 netic field, the acceptor LDOS is essentially identical to  
 474 the one calculated in the absence of the field, in agree-  
 475 ment with the experimental results.

476 Before continuing our LDOS analysis, it is useful to  
 477 consider how the anisotropy-energy barrier depends on  
 478 the Mn-impurity depth from the (110) surface. In Fig. 6  
 479 we plot the largest value of the anisotropy energy barrier  
 480 as a function of the subsurface layer index (layer 0 is the  
 481 (110) surface). In general, in the absence of a magnetic  
 482 field (red dots in the picture) the anisotropy barrier in-  
 483 creases with Mn depth, reaching a maximum of 15 meV  
 484 for layers 4 and 5. It then starts to decrease and it should  
 485 eventually reach a very small value corresponding to the  
 486 case where the Mn is effectively in the bulk. For the finite  
 487 clusters that we have considering here (20 layers in the  
 488 z-direction), the anisotropy remains large also when the  
 489 impurity is effectively in the middle of the cluster (corre-  
 490 sponding to layer 9 from the surface). Bulk calculations  
 491 on considerably larger clusters show that the anisotropy  
 492 for impurities in the middle of the clusters does decrease  
 493 to a fraction of one meV[19]. For these larger clusters  
 494 the magnetic anisotropy of the Mn positioned in on lay-  
 495 ers  $\geq 8$  is expected to decrease a bit with cluster size.  
 496 However the qualitative behavior of the first 7-8 layers  
 497 shown in Fig. 6, and the corresponding numerical values  
 498 of the magnetic anisotropy are controlled by the vicinity  
 499 to the surface and as such should not depend strongly on  
 500 cluster size[19].

501 Layer 1 (the first subsurface layer) is a special case in  
 502 the sense that the anisotropy is very small, on the or-

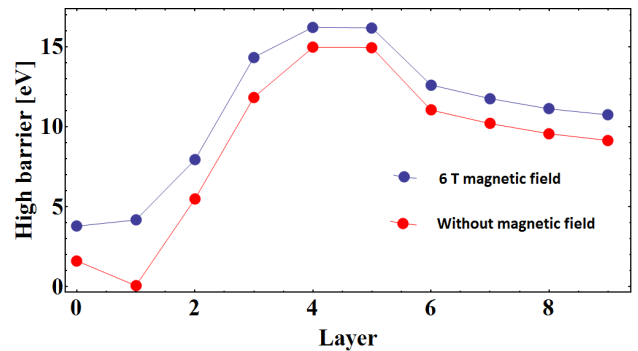


FIG. 6. Color online – The maximum MAE barrier height as a function of the Mn depth. Red dots are the MAE barrier height in the absence of an external magnetic field, while blue dots represent the height in the presence of a 6 T external magnetic field.

503 der of 0.1 meV. The first subsurface represents the cross  
 504 over from the case in which the Mn is at the surface,  
 505 with three nearest neighbor As, to a bulk-like environ-  
 506 ment characterized by four nearest neighbor As atoms.  
 507 The properties of the acceptor level found in STM exper-  
 508 iments for a Mn positioned on this subsurface are also  
 509 quite anomalous[35]. When a magnetic field of 6 T is  
 510 applied along the hard direction (blue dots in Fig. 6)  
 511 the anisotropy barrier increases by a couple of meV. The  
 512 exception is again the first subsurface (layer 1), whose  
 513 anisotropy is now completely controlled by the magnetic  
 514 field and behaves in a similar way to the surface layer.  
 515 The behavior of the first subsurface anisotropy landscape  
 516 is shown explicitly in Fig. 7 (a), (d).

517 As for the case of a Mn atom placed at the (110) sur-  
 518 face, the acceptor LDOS for a Mn on the first subsurface  
 519 (see Fig. 7(b), (c) ) is completely insensitive to the direc-  
 520 tion of the Mn magnetic moment. Again a 6 T magnetic  
 521 field, which is able to completely modify the magnetic  
 522 anisotropy landscape and orient the Mn moment parallel  
 523 to its direction, does not have any detectable effect on  
 524 the acceptor wave function, as shown in Fig. 7(d).

525 As the Mn is placed in successively deeper layers below  
 526 the surface and the acceptor wavefunction becomes less  
 527 localized around the impurity, the situation changes. In  
 528 Figs. 8 and 9 we plot the anisotropy landscape and the  
 529 acceptor LDOS for the fourth and fifth subsurface (layer  
 530 4 and 5 below the surface) respectively. As we discussed  
 531 before, when the direction of the Mn moment is forced  
 532 to point in the hard direction (panel (c) of Fig. 8) the  
 533 LDOS around the Mn increases sensibly. The two cases,  
 534 easy (panel b) and hard axis LDOS are now clearly dis-  
 535 tinguishable. Since the acceptor wavefunction is always  
 536 normalized, an increase of the LDOS in the core region  
 537 implies that the acceptor wavefunction is considerably  
 538 more localized when the Mn magnetic moment points in  
 539 the hard direction. On the other hand, in contrast to  
 540 the surface and the first subsurface, the energy barrier in  
 541 this case is considerably larger. A magnetic field of the

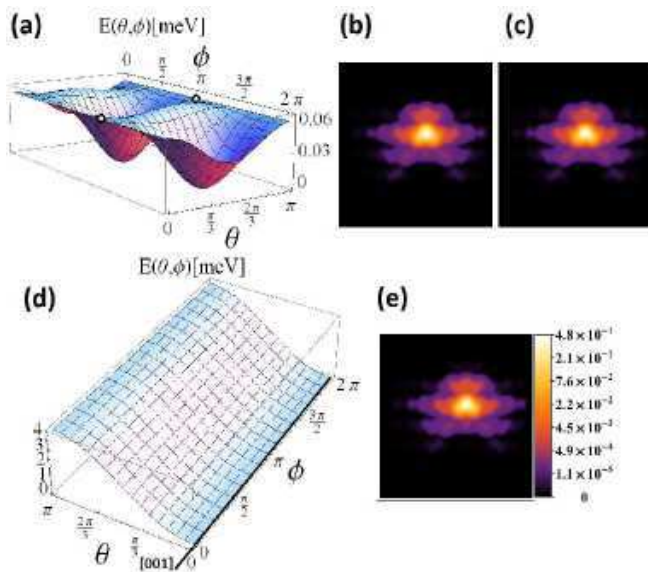


FIG. 7. The MAE landscape and the Mn-acceptor-level LDOS for one Mn in the first subsurface (i.e., one layer below the [110] surface). (a) The MAE in the absence of an external magnetic field. The barriers (hard) directions are marked with a circle. (b) and (c) the Mn acceptor LDOS for the case in which the Mn magnetic moment points in the easy and hard direction respectively. (d) The MAE in the presence of a 6 T external magnetic field pointing along the (original) hard direction ( $\theta = 0, \phi = \pi$ ). The minimum energy (easy direction) is shown with a solid line. (e) The Mn acceptor LDOS in the presence of a 6 T magnetic field. Here the Mn magnetic moment points in the new easy direction determined by the magnetic field, as shown in (d). The colorscale in (b) and (c) is the same as in (e).

542 order of those applied experimentally are now not strong  
 543 enough to modify appreciably the anisotropy landscape.  
 544 This can be seen by comparing panel (a) – no magnetic  
 545 field – with panel (d), where magnetic field of 6 T is applied  
 546 in the hard direction. Consequently, the direction of  
 547 the easy axis is only slightly modified in the presence of a  
 548 magnetic field, and as a result, the corresponding accep-  
 549 tor LDOS appears now very similar to the zero-magnetic  
 550 field case [panel (b)]. This is again in agreement with the  
 551 experiments presented in this paper.

552 As mentioned before, the experiments presented in [14]  
 553 showed the energy level splitting of Mn in GaAs close to  
 554 the cleavage surface. For a typical Mn position at 5th  
 555 subsurface layer, a total splitting of 14 meV is found be-  
 556 tween the 3 peaks which are attributed to the different  
 557 projections of the total momentum  $J=1$  which is the re-  
 558 sult of anti-ferromagnetic coupling between the  $5/2$  Mn  
 559 core spin and  $3/2$  Mn acceptor total angular momentum.  
 560 In Fig. 9, it can be seen that the MAE is indeed about  
 561 15 meV which corresponds well with the findings in [14].  
 562 In Fig. 1, the MAE as calculated in another tight bind-  
 563 ing calculation (strained bulk GaAs) is about 23 meV.  
 564 This is more than the 15 meV of the supercell calcula-  
 565 tions (Fig. 9) possibly because of the overestimated

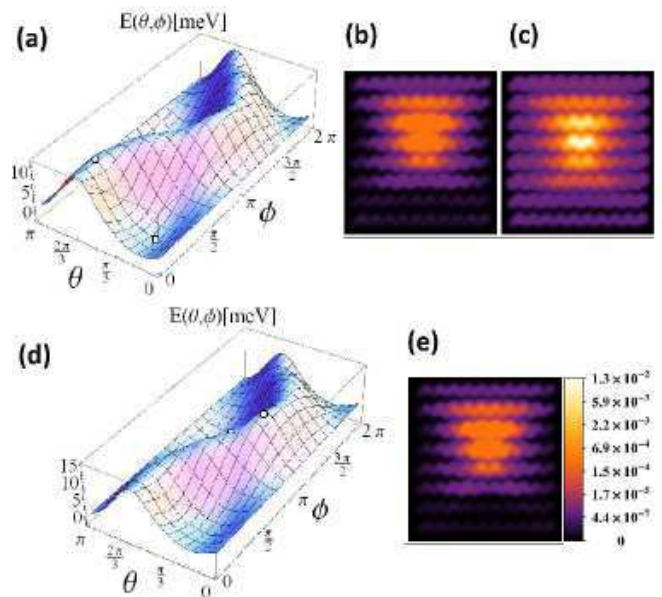


FIG. 8. The magnetic anisotropy energy (MAE) and the LDOS for one Mn in the fourth subsurface (fourth layer below the [110] surface). (a) The MAE in the absence of an external magnetic field. (b) and (c) the LDOS of Mn acceptor level for the case that Mn magnetic moment points in the easy and hard direction respectively. (d) The MAE in the presence of a 6 T external magnetic field which points along the hard direction ( $\theta = \pi/2, \phi = 3\pi/4$ ). (e) The LDOS in the case that magnetic moment points in the easy direction in the presence of a 6 T magnetic field. The barrier direction in (a) and (d) is marked with a circle and the easy direction with a square. The colorscale in (b) and (c) is the same as in (e).

566 strain or its assumed uniformity.

567 We conclude that, although the LDOS of deep-  
 568 subsurface Mn acceptors is in principle strongly depend-  
 569 ent on the Mn magnetic moment direction, its actual  
 570 manipulation with an external magnetic field is not suit-  
 571 able at field strengths presently used in experiment.

## 572 VI. CONCLUSIONS

573 In conclusion, this work is the first systematic study  
 574 of the effect of an external applied magnetic field on the  
 575 acceptor properties of individual Mn impurities in GaAs.  
 576 Specifically, we have investigated theoretically and ex-  
 577 perimentally the effect of an external magnetic field on  
 578 the acceptor hole wavefunction and LDOS of Mn impuri-  
 579 ties placed near the (110) surface of GaAs. The acceptor  
 580 LDOS is directly accessible via X-STM experiments.

581 The motivation of this study was in part provided  
 582 by previous theoretical studies which predicted that the  
 583 LDOS in some cases strongly depends on the orientation  
 584 of the magnetic impurity magnetic moment. The theoret-  
 585 ically model used in this analysis is essentially parameter-  
 586 free, once the energy of the surface acceptor state is fixed  
 587 to reproduce the experimental value.



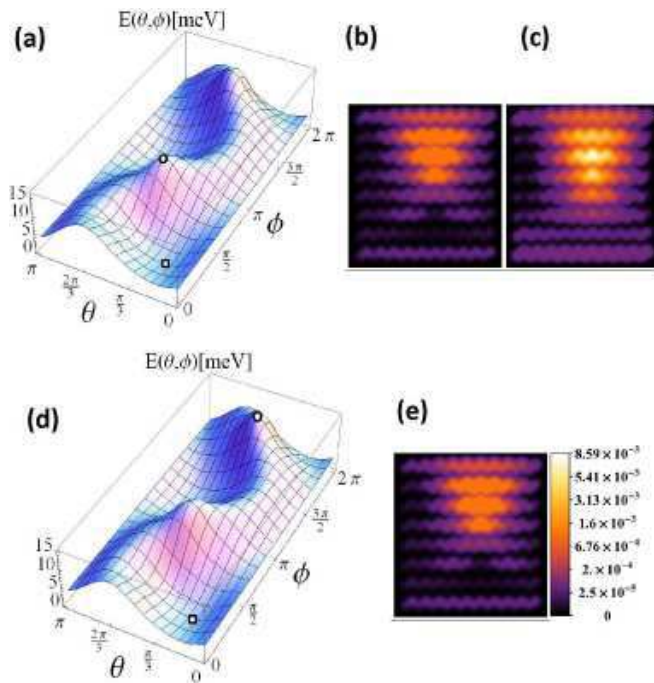


FIG. 9. As in Fig. 8, but for the fifth subsurface (fifth layer below the [110] surface). The colorscale in (b) and (c) is the same as in (e).

588 Experimentally we find that there is no detectable dif-  
 589 ference in the STM images of the acceptor hole LDOS  
 590 when a magnetic field up to 6 T is applied in several  
 591 directions with respect to the crystal structure. To re-  
 592 concile theory and experiment we have carried out a the-  
 593 oretical analysis of the magnetic anisotropy energy and  
 594 acceptor hole wavefunction in the presence of a magnetic  
 595 field. We have shown that for Mn impurities placed in  
 596 deep sub-layers below the surface, the calculated mag-  
 597 netic anisotropy landscape is characterized by energy  
 598 barriers of the order of 10-20 meV, which are only mini-  
 599 mally affected by magnetic fields used in experiment. We  
 600 estimate that one needs to employ much stronger fields  
 601 (on the order of tens of Tesla) to modify significantly the  
 602 anisotropy landscape and rotate the magnetic moment  
 603 of the impurity. This estimate is based on the idea of  
 604 manipulating a spin=5/2 object with g-factor=2 with an  
 605 external field to overcome an energy barrier of 15 meV.  
 606 For impurities placed near the surface, the magnetic

607 anisotropy is small enough to be considerably affected by  
 608 a magnetic field of a few T. However, for this case the ac-  
 609 ceptor hole LDOS is much less sensitive to the orientation  
 610 of the Mn magnetic moment. The combination of these  
 611 two facts seem to explain the experimental finding that  
 612 the the STM images of the acceptor hole wavefunction is  
 613 essentially unaffected by an external magnetic field.

614 Our studies show that the Mn-dopant behavior close  
 615 to the GaAs surface depends on the layer depth in a  
 616 complex and highly non trivial way. These studies also  
 617 suggest that it could be interesting to carry out a sim-  
 618 ilar investigation for other magnetic dopants and other  
 619 semiconductors. It might be possible that for some of  
 620 these systems the acceptor wavefunction for a dopant  
 621 near the surface be more delocalized and amenable to an  
 622 easier manipulation by a static magnetic field, display-  
 623 ing the effects originally predicted for Mn in GaAs. It  
 624 should also be possible to use resonant techniques, such  
 625 as those commonly used in electron spin resonance and  
 626 ferromagnetic resonance, to map out the anisotropy land-  
 627 scape presented here for Mn near the GaAs surface. Fi-  
 628 nally, excitations of the spin that would correspond to the  
 629 quantized spin in the anisotropy landscape here should  
 630 be visible in inelastic tunneling spectroscopy. Thus these  
 631 new predictions do not mean that Mn spin dynamics is  
 632 impossible to see near the surface of GaAs, merely that  
 633 it is more challenging to observe.

## ACKNOWLEDGMENTS

635 We would like to thank W. van Roy and Z. Li for  
 636 the Mn doped GaAs samples which they have provided  
 637 and A. H. MacDonald for several useful discussions. We  
 638 would like to thank also B. Bryant for substantial exper-  
 639 imental support during the X-STM measurements.  
 640 This work was supported by STW-VICI Grant No.  
 641 6631. We acknowledge support from the Engineering and  
 642 Physical Sciences Research Council (EPSRC) through  
 643 grants EP/D063604/1 (PS, SRS, NJC, and CFH) and  
 644 EP/H003991/1 (SRS). This work was also supported in  
 645 part by the Faculty of Natural Sciences at Linnaeus Uni-  
 646 versity, by the Swedish Research Council under Grant  
 647 Numbers: 621-2007-5019 and 621-2010-3761 and by the  
 648 Nordforsk research network: 08134, *Nanospintronics:*  
 649 *theory and simulations.*

- 
- 650 [1] I. Karlik, I. Merkulov, D. Mirlin, L. Nikitin, V. Perel, 658  
 651 and V. Sapega, *Sov. Phys. Solid State* **24**, 2022 (1982). 659  
 652 [2] T. Dietl, H. Ohno, and F. Matsukura, 660  
 653 *Phys. Rev. B* **63**, 195205 (2001). 661  
 654 [3] T. Jungwirth, K. Y. Wang, J. Mašek, K. W. Edmonds, 662  
 655 J. Knig, J. Sinova, M. Polini, N. A. Goncharuk, A. H. 663  
 656 MacDonald, M. Sawicki, A. W. Rushforth, R. P. Cam- 664  
 657 pion, L. X. Zhao, C. T. Foxon, , and B. L. Gallagher, 665  
 658 *Phys. Rev. B* **72**, 165204 (2005).  
 659 [4] R. Myers, M. Mikkelsen, J.-M. Tang, A. Gossard,  
 660 M. Flatté, and D. Awschalom, *Nature Materials* **7**, 203  
 661 (2008).  
 662 [5] A. Kudelski, A. Lemaitre, A. Miard, P. Voisin, T. Gra-  
 663 ham, R. Warburton, and O. Krebs, *Phys. Rev. Lett.* **99**,  
 664 247209 (2007).  
 665 [6] Y. Léger, L. Besombes, J. Fernández-Rossier, L. Main-

- 666 gault, and H. Mariette, Phys. Rev. Lett. **97**, 107401  
667 (2006).
- 668 [7] G. Fuchs, G. Burkard, P. Klimov, and D. Awschalom,  
669 Nature Physics **7**, 789 (2011).
- 670 [8] A. M. Yakunin, A. Y. Silov, P. M. Koenraad, W. V. Roy,  
671 J. D. Boeck, J.-M. Tang, and M. E. Flatté, Phys. Rev.  
672 Lett **92**, 216806 (2004).
- 673 [9] J.-M. Tang and M. Flatté, Phys. Rev. Lett. **92**, 047201  
674 (2004).
- 675 [10] A. M. Yakunin, A. Y. Silov, P. M. Koenraad, J.-M. Tang,  
676 M. E. Flatté, J.-L. Primus, W. V. Roy, J. D. Boeck, A. M.  
677 Monakhov, K. S. Romanov, I. E. Panaiotti, and N. S.  
678 Averkiev, Nat. Mater. **6**, 512 (2007).
- 679 [11] C. Çelebi, J. K. Garleff, A. Y. Silov, A. M. Yakunin,  
680 P. M. Koenraad, W. V. Roy, J.-M. Tang, and M. E.  
681 Flatté, Phys. Rev. Lett. **104**, 086404 (2010).
- 682 [12] J.-M. Tang and M. E. Flatté, Phys. Rev. B **72**, 161315  
683 (2005).
- 684 [13] T. O. Strandberg, C. M. Canali, and A. H. MacDonald,  
685 Phys. Rev. B **80**, 024425 (2009).
- 686 [14] J. Garleff, A. Wijnheijmer, A. Silov, J. van Bree, W. V.  
687 Roy, J.-M. Tang, M. E. Flatté, and P. Koenraad, Phys.  
688 Rev. B **82**, 035303 (2010).
- 689 [15] M. S. Grinolds, P. Maletinsky, S. Hong, M. D. Lukin,  
690 R. L. Walsworth, and A. Yacoby, Nat. Phys **7**, 687  
691 (2011).
- 692 [16] D. Kitchen, A. Richardella, J.-M. Tang, M. E. Flatté,  
693 and A. Yazdani, Nature **442**, 436 (2006).
- 694 [17] D.-H. Lee and J. A. Gupta, Nano Lett. **11**, 2004 (2011).
- 695 [18] J. Schneider, U. Kaufmann, W. Wilkening, M. Baeumler,  
696 and F. Köhl, Phys. Rev. Lett. **59**, 240 (1987).
- 697 [19] M. R. K. Mahani and C. M. Canali, Unpublished Results  
698 (2011).
- 699 [20] J. C. Slater and G. F. Koster, Phys. Rev. **94**, 1498 (1954).
- 700 [21] D. A. Papaconstantopoulos and M. J. Mehl, J. Phys.:  
701 Cond. Mat. **15**, R413 (2003).
- 702 [22] D. J. Chadi, Phys. Rev. B **16**, 790 (1977).
- 703 [23] D. J. Chadi, Phys. Rev. Lett. **41**, 1062 (1978).
- 704 [24] D. J. Chadi, Phys. Rev. B **19**, 2074 (1979).
- 705 [25] C. Timm and A. H. MacDonald, Phys. Rev. B **71**, 155206  
706 (2005).
- 707 [26] H. Ohno, Science **281**, 951 (1998).
- 708 [27] K. Teichmann, M. Wenderoth, S. Loth, R. G. Ulbrich,  
709 J. K. Garleff, A. P. Wijnheijmer, and P. M. Koenraad,  
710 Phys. Rev. Lett. **101**, 076103 (2008).
- 711 [28] W. Schairer and M. Schmidt, Phys. Rev. B **10**, 2501  
712 (1974).
- 713 [29] T. Lee and W. W. Anderson, Solid State Commun. **2**,  
714 265 (1964).
- 715 [30] R. A. Chapman and W. G. Hutchinson, Phys. Rev. Lett.  
716 **18**, 443 (1967).
- 717 [31] M. Linnarsson, E. Janzen, B. Monemar, M. Kleverman,  
718 and A. Thilderkvist, Phys. Rev. B **55**, 6938 (1997).
- 719 [32] J. K. Garleff, C. Çelebi, W. van Roy, J.-M. Tang, M. E.  
720 Flatté, and P. M. Koenraad, Phys. Rev. B **78**, 075313  
721 (2008).
- 722 [33] Because the electron charge is negative, magnetic mo-  
723 ments and angular momentum are in fact oriented an-  
724 tiparallel to each other. In a magnetic field the energeti-  
725 cally favorable direction of the magnetic moment is par-  
726 allel to the field while the direction of the spin is an-  
727 tiparallel. Assuming that magnetic moment and angular  
728 momentum are parallel is strictly speaking incorrect but  
729 does not change the physics.
- 730 [34] M. F. Islam and C. M. Canali, Phys. Rev. B **85**, 155306  
731 (2012).
- 732 [35] D. H. Lee and J. A. Gupta, Science **330**, 1807 (2010).